Dalton Transactions

A Ru(II)-Arene-Ferrocene Complex With Promising Antibacterial Activity

Journal:	*Dalton Transactions*
Manuscript ID	DT-ART-08-2022-002696.R1
Article Type:	Paper
Date Submitted by the Author:	26-Oct-2022
Complete List of Authors:	Mensah, Stephen; Illinois State University, Department of Chemistry Rosenthal, Joseph; Illinois State University, Department of Chemistry Dagar, Mamta; University of Rochester, Department of Chemistry Brown, Tyson; Illinois State University, Department of Chemistry Mills, Jonathan; Illinois State University, Department of Chemistry Hamaker, Christopher; Illinois State University, Department of Chemistry Ferrence, Gregory; Illinois State University, Department of Chemistry Webb, Michael; SUNY Geneseo, Department of Chemistry; Illinois State University, Department of Chemistry

ARTICLE

A Ru(II)-Arene-Ferrocene Complex With Promising Antibacterial Activity

Stephen Mensah,[a] Joseph D. Rosenthal,[a] Mamta Dagar,[c] Tyson Brown,[a] Jonathan J. Mills,[a] Christopher G. Hamaker,[a] Gregory M. Ferrence,[a] Michael I. Webb[a,b]*

Received 00th January 20xx,
Accepted 00th January 20xx

DOI: 10.1039/x0xx00000x

The evolution of high virulence bacterial strains has necessitated the development of novel therapeutic agents to treat resistant infections. Metal-based therapeutics represent a promising avenue for advancement, given their structural variability and unique modes of action relative to classical organic molecules. One strategy that has seen marked success is the incorporation of ferrocene into the framework of established antibacterial agents, while ruthenium-based complexes have also shown promise as bioactive compounds. This work focused on the preparation of novel ruthenium(II)-arene complexes containing Schiff base ligands with an attached ferrocene, and evaluation of their antibacterial activity. Structure-activity relationships identified the importance of having a phenyl group between the Schiff base imine and the appended ferrocene. This complex, **C2**, showed prominent activity against several clinically relevant bacterial strains, including a minimum inhibitory concentration of 16 μg/mL for methicillin-resistant *Staphylococcus aureus* (MSRA). Overall, the results of this study represent a promising new lead for future development of novel antibacterial agents.

Introduction,

There is currently an arms race to counteract the evolution of resistant bacterial strains through the development of novel therapeutic treatments. This antibiotic-resistance crisis has several causative factors, including the overuse and misuse of medications, along with the lack of new drug developments.[1, 2] In the United States, over 2.8 million people are infected with antibiotic-resistant infections annually, resulting in 35,000 deaths.[3] This represents a critical need in the field of drug discovery, in particular, the development of novel therapeutic scaffolds for evaluation, rather than derivatives of established families of compounds.

Metal-based complexes represent an auspicious avenue for antibacterial development, as the coordination environment around the metal center offers stereochemical variability not available with conventional organic complexes.[4] Several metal complexes have been used in medicine throughout history, beginning with arsenic, which was used to treat ulcers by Hippocrates.[5] Centuries later, the arsenic-containing compound Salvarsan became the first synthetic antibiotic for the treatment of syphilis.[6] Since the serendipitous discovery of cisplatin and its subsequent clinical success,[7, 8] metallotherapeutics have been extensively investigated as anticancer agents.[9] Unfortunately, the use of metal-based complexes as antibacterial candidates has not seen the same interest.[10]

Among the transition metals, ruthenium-based complexes have seen substantial success as therapeutic agents given their desirable pharmaceutical properties including relatively slow rates of ligand exchange, several physiologically accessible oxidation states, and iron-mimicry.[11, 12] One class of ruthenium complexes that has been extensively studied are Ru(II) complexes which adopt a "piano-stool" configuration. Here, one face of the metal center is occupied by a coordinated η^6-arene ring, while the other side contains the remaining 3 ligands to complete the octahedral coordination sphere.[13] The overall formula for such complexes is [(η^6-arene)-Ru(X)(Y)(Z)], where the variable ligands give rise to two distinct families of Ru(II) complexes. The first family was developed by the group of Peter Sadler,[14, 15] and are modeled after the lead complex RM175 (**Figure 1**).[16] Ru-arene complexes of this family commonly incorporate a bidentate nitrogen or oxygen donor ligand, while the remaining coordination site is occupied by a halogen. This results in a positive complex ion, where charge compensation is typically provided by hexafluorophosphate or a halogen. These complexes have demonstrated cytotoxic activity *in vitro,* where the principal target is DNA.[17, 18] The other family of Ru(II) complexes was developed by the group of Paul Dyson, where a hallmark of this family is the inclusion of a 1,3,5-triaza-7-phosphaadamantane (PTA) ligand.[19, 20] Such complexes often have 3 monodentate ligands, 2 of which are anionic, resulting in a neutral coordination complex.[21] This family is known as the RAPTA family of complexes,[22] for which the lead candidate RAPTA-C (**Figure 1**), has displayed modest cytotoxicity *in vitro*,[23] while recent studies have shown tumor reduction *in vivo*.[24] The therapeutic success of these two families of Ru(II) complexes led to the exploration of Ru(II) complexes as potential antibacterial candidates, given their promising biological activity.

[a] *Department of Chemistry, Illinois State University, Normal, IL, 61790*
[b] *Department of Chemistry, SUNY Geneseo, Geneseo, NY, 14454*
c Department of Chemistry, University of Rochester, Rochester, NY, 14627
Corresponding Author: Michael I. Webb, mwebb@geneseo.edu
Electronic Supplementary Information (ESI) available: ^{1}H NMR, ^{13}C NMR, CV, UV-Vis, HSA fluorescence, DNA titration, and X-ray crystallographic information. See DOI: 10.1039/x0xx00000x

Previous examples of ruthenium antibacterial compounds have been dominated by coordinatively saturated complexes with aromatic ligands such as 1,10-phentheoline and its derivatives.[25] Such polypyridylruthenium(II) complexes interact predominately with DNA via non-coordinative intercalation which is aided by an electrostatic attraction.[26] Alternatively, the use of Ru-arene complexes containing Schiff base ligands as antimicrobial agents is a promising avenue for advancement given the versatile and modular nature of the ligand preparation.[27]

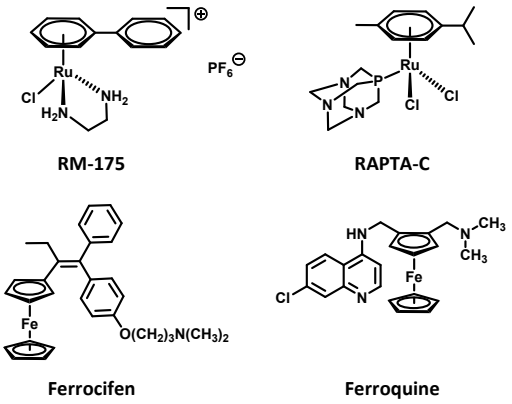

Figure 1. The anticancer Ru(II)-arene compounds RM175 and RAPTA-C, along with the ferrocene-incorporated drugs Ferrocifen and Ferroquine.

The incorporation of ferrocene (Fc) into biologically active compounds began with the preparation of ferroquine (**Figure 1**) from chloroquine, which exhibited potent antimalarial activity.[28] This was followed almost immediately by the ferrocene-based derivative of the breast cancer drug tamoxifen, creating ferrocifen (**Figure 1**), which itself displayed improved anticancer activity relative to its parent compound.[29] These seminal discoveries established the use of ferrocene in the synthesis of novel therapeutic compounds, establishing a new class of therapeutics, called ferrocifens,[30] where ferrocene is actively incorporated into a pharmaceutical.[31] Indeed, ferroquine has also been recently observed to possess antitumor activity,[32] demonstrating the diverse biological activity that can be unleashed via the incorporation of a ferrocene functional group. Previous derivatives of RAPTA-C where the PTA was exchanged for a heterocyclic ligand containing a conjugated ferrocene demonstrated both antiproliferative and antibacterial properties.[33] Given the established biological activity of ferrocene-based compounds, our target Ru-arene complexes were prepared using Schiff base ligands that contained a conjugated ferrocene (**Figure 2**). These novel complexes were evaluated for their stability, DNA and protein binding behavior, and ultimately their antibacterial efficacy against several clinically relevant strains. From these studies, preliminary structure-activity relationships (SAR) for the impact of the Fc, and its proximity to the ruthenium metal center, were determined.

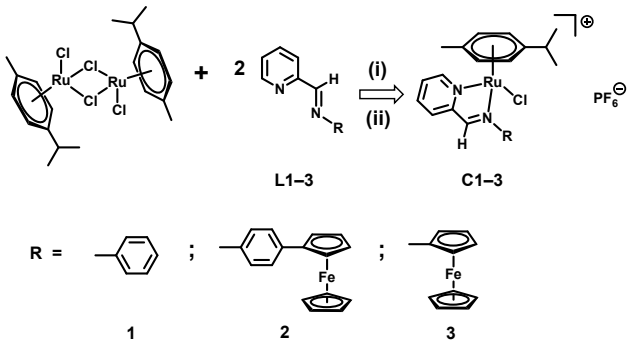

Figure 2. The Ru(II)-arene complexes prepared and evaluated in this report. Experimental conditions (i) MeOH, 4h, RT, and (ii) NH_4PF_6 (5 eq), 10 minutes.

Experimental

Unless otherwise noted, all reagents and materials were used as received. The reagents utilized were purchased from Fisher Scientific, Sigma Aldrich, Cambridge Isotope Laboratories or Oakwood Chemical. Human serum albumin (HSA) and calf-thymus DNA (CT-DNA) were acquired from Sigma Aldrich as lyophilized powders.

The ^{1}H NMR in $CDCl_3$ were collected using a Bruker Avance III 400 MHz NMR spectrometer, while the ^{1}H NMR in DMSO/D_2O and the ^{13}C NMR were collected using a Varian 400-MR 400 MHz NMR Spectrometer. UV-Vis spectra were collected using an Evolution 260 Bio Spectrophotometer equipped with a single cell Peltier system and a Haake DC 10 pump. Fluorescence measurements were conducted using a Varioskan LUX plate reader.

Aminoferrocene,[34] ferrocenylaniline,[35, 36] **L1**,[37] **L2**,[38] **L3**,[39] and the Ru(II)-arene dimer[40] ([Ru(*p*-cymene)Cl_2]$_2$) were all prepared following previous procedures.

General Conditions for the Synthesis of C1-C3

The prepared Ru(II)-arene dimer (0.35 mmol) and **L1-3** (0.70 mmol) were combined in methanol (8 mL) and the resulting mixture was stirred at room temperature for 4 hours. Ammonium hexafluorophosphate (3.5 mmol) was then added directly and stirring continued for 10 minutes. The reaction mixture was then stored in the fridge overnight and solid precipitates formed. The solid product was then isolated by vacuum filtration and dried under high vacuum for several hours.

Compound C1

Bright orange solid. Yield: 83 % Crystals suitable for X-ray diffraction were grown from the reaction filtrate following extended cooling at −20 °C. ^{1}H NMR δ = (400 MHz, $CDCl_3$): 9.34 (d, 1H), 8.44 (s, 1H), 8.10 (t, 1H), 7.83 (d, 1H), 7.76 (dd, 7.58 (m, 1H), 5.74 (d, 2H), 5.48 (d, 2H), 5.43 (dd, 2H), 2.7 (sep, 1H), 2.19 (s, 3H), 1.21 (d, 3H), 1.16 (d. 3H). ^{13}C NMR δ = (100 MHz, $CDCl_3$): 18.74, 21.93, 22.42, 31.17, 85.40, 86.13, 87.04, 122.60, 129.68,

130.27, 130.70, 152.10, 154.48, 156.46, 166.70. Elemental Analysis (C, H, N, weight % $C_{22}H_{24}ClRuPF_6 \bullet H_2O$): Theoretical: 42.90 % C, 4.25 % H, 4.55 %N. Experimental: 43.12 % C, 3.89 % H, 4.69 % N.

Compound C2

Dark purple solid. Yield: 53 % ^{1}H NMR δ = (400 MHz, $CDCl_3$): 9.30 (s, 1H), 8.22 (d, 1H), 8.05 (t, 1H), 7.70 (t, 1H), 5.88 (d, 1H), 5.49 (t, 2H), 5.37 (d, 2H), 4.84 (s, 2H), 4.55 (d, 2H), 4.29 (s, 5H), 2.61 (sep, 1H), 2.24 (s, 3H), 1.13 (d, 3H), 1.07 (d. 3H). ^{13}C NMR δ = (100 MHz, D_6-DMSO): 18.71, 22.02, 22.14, 30.91, 67.01, 67.24, 70.08, 70.16, 83.33, 85.53, 85.71, 86.67, 86.89, 103.67, 105.45, 123.21, 126.74, 129.15, 130.21, 149.71, 155.17, 156.42, 166.99. Elemental Analysis (C, H, N, weight % $C_{32}H_{32}N_2ClFeRuPF_6 \bullet H_2O$): Theoretical: 48.05 % C, 4.28 % H, 3.50 %N. Experimental: 48.28 % C, 3.93 % H, 3.70 % N.

Compound C3

Dark green solid. Yield: 72 % Crystals suitable for X-ray diffraction were grown following vapor diffusion of pentane into acetone. ^{1}H NMR δ = (400 MHz, $CDCl_3$): 9.31 (d, 1H), 8.48 (s, 1H), 8.1 (t, 1H), 7.75 (t, 1H), 7.64 (d, 1H), 5.76 (d, 2H), 5.52 (d, 2H), 5.45 (d, 2H), 4.78 (s, 2H), 4.49 (s, 2H), 4.12 (s, 5H), 2.76 (sep, 1H), 2.21 (s, 3H), 1.22 (d, 3H), 1.17 (d. 3H). ^{13}C NMR δ = (100 MHz, D_6-DMSO): 18.85, 22.06, 30.94, 67.09, 68.27, 68.69, 69.19, 84.46, 84.79, 86.95, 87.31, 104.55, 106.82, 128.28, 129.40, 140.35, 155.02, 156.55, 165.83. Elemental Analysis (C, H, N, weight % $C_{26}H_{28}N_2ClFeRuPF_6$): Theoretical: 44.24 % C, 4.00 % H, 3.97 %N. Experimental: 43.92 % C, 3.90 % H, 4.01 % N.

Log $D_{7.4}$

To ensure complete dissolution, the complexes were first mixed with dimethyl sulfoxide (DMSO), then immediately diluted using phosphate buffered saline (PBS, pH 7.4) to achieve a final DMSO concentration of 1%. The absorbance spectrum of the aqueous solution prior to mixing was measured, then an equal volume of 1-octanol was added, and the two phases were mixed using an IKA Trayster digital mixer under ambient conditions for 2 hours. After mixing, the samples were briefly centrifuged (3 minutes, 2200 g) and the aqueous layer was carefully removed, and its absorbance spectrum was measured. The log $D_{7.4}$ value for each complex was then determined using the following equation:

$$Log\ D_{7.4} = log\left(\frac{Abs\ at\ \lambda_{max}\ before\ mixing}{Abs\ at\ \lambda_{max}\ after\ mixing} - 1\right)$$

Cyclic Voltammetry

Cyclic voltammetry was performed using a three-electrode setup inside a nitrogen filled glove box (Vigor Tech, USA) using a Bio-Logic SP 150 potentiostat/galvanostat and the EC-Lab software suite. The concentrations of **C1-3** were kept at 1 mM and 100 mM of [^{n}Bu$_4$N][PF_6] was used throughout all measurements. Cyclic voltammograms were recorded using a 3 mm diameter glassy carbon working electrode (CH Instruments, USA), a Pt wire auxiliary electrode (CH Instruments, USA), and an Ag/Ag$^+$ non-aqueous reference electrode with 0.01 M $AgNO_3$ in 0.1 M [^{n}Bu$_4$N][PF_6] in MeCN (BASi, USA). Ferrocene was used as the internal standard for **C1**, whereas decamethylcobaltocene was used for **C2** and **C3**. The latter two complexes were later externally referenced to the Fc^+/Fc couple. Cyclic voltammograms were iR compensated at 85% with impedance taken at 100 kHz using the ZIR tool included within the EC-Lab software.

UV-Vis Sample Preparation

Aqueous samples of **C1**-**C3** were prepared at a concentration of 100 μM by dissolving the complexes in a 10% DMSO and PBS (pH 7.4) solution. UV-Vis spectra of the complexes were collected every 10 minutes over a period of 6 hours using a Thermo Scientific Evolution 260 Bio Spectrophotometer. The sample temperature was maintained at 37 °C using a single cell Peltier system.

Human Serum Albumin Binding Assay

A stock solution of human serum albumin (HSA) was prepared fresh using PBS (pH 7.4). Additional stock solutions of each of the Ru(II) complexes were also prepared using 10% DMSO in PBS. For the assay, aliquots from both stock solutions were combined to afford HSA:Ru ratios from 1:1 to 1:10. These were plated onto a 96 well plate in triplicate and incubated for one hour at 37 °C, after which fluorescence measurement were taken where the excitation wavelength was set at 280 nm and the emission spectra were collected at 299 nm to 600 nm.

DNA Binding Assay

Calf-thymus deoxyribonucleic acid (CT-DNA) was dissolved in 50 mM tris-HCl buffer (pH 7.0) where the concentration of the sample was determined by measuring the absorbance at 280 nm and using the extinction coefficient of 6600 M^{-1} cm^{-1}.[41] Additional measurement of the absorbance ratio at 260/280 nm gave a value of ~1.9, which is indicative of the sample being relatively free of protein.[42] Absorbance titrations were performed using a fixed concentration of the Ru complexes (30 uM) and a gradually increasing concentration of CT-DNA (0 to 90 uM). The samples were incubated for 1 hour at 37 °C prior to analysis.

The intrinsic binding constant (K_b) for each Ru complex to CT-DNA was obtained using the following equation:

$$[DNA] / (\varepsilon_A - \varepsilon_F) = [DNA] / (\varepsilon_B - \varepsilon_F) + 1 / K_b(\varepsilon_B - \varepsilon_F)$$

where ε_A corresponds to A_{obs} / [Ru], ε_F is the extinction coefficient of the free Ru complex, and ε_B is the extinction coefficient for the Ru complex in the fully bound form. To determine the K_b for each Ru complex, a plot of [DNA] / ($\varepsilon_A - \varepsilon_F$) versus [DNA] was prepared where the ratio of the slope to the y-intercept gave the binding constant.[43, 44]

Minimum Inhibitory Concentration Assays

Minimum inhibitory concentrations (MICs) were determined by broth micro-dilution according to Clinical & Laboratory

Standards Institute guidelines.[45] The test medium was lysogeny broth (LB). *Staphylococcus aureus* (ATCC 25923), methicillin-resistant *Staphylococcus aureus* (MRSA, ATCC 33591), MRSA (ATCC BAA-44), *Staphylococcus epidermidis* (ATCC 51625), *Enterococcus faecalis* (ATCC 51299), *Pseudomonas aeruginosa* (ATCC 27853), and *Acinetobacter baumannii* (ATCC 19606) were grown in LB for 6–8 hr; this culture was then used to inoculate fresh LB (5×10^5 CFU/mL). The resulting bacterial suspension was aliquoted (1 mL) and compound was added from a 10 mM DMSO stock to achieve the desired initial starting concentration (128 µg/mL). Linezolid or amikacin (from a 10 mM DMSO stock) was used as a positive control with final concentrations ranging from 0.063 to 128 µg/mL. Inoculated media not treated with compound served as the negative control. The plate was incubated under stationary conditions at 37°C. After 16 hours, MIC values were recorded as the lowest concentration of the compound at which no visible growth of bacteria was observed, based on duplicate plates performed in three separate experiments.

Red Blood Cell Hemolysis Assay

The red blood cell hemolysis assay was performed on mechanically defibrinated sheep blood (Hemostat Labs: DSB50). Defibrinated blood (1.5 mL) was placed in a microcentrifuge tube and centrifuged for 10 minutes at 2,000 *g*. The supernatant was then removed, and the pelleted cells were resuspended in 1 mL of PBS. The resulting suspension was centrifuged again for 10 minutes at 2,000 *g*. The supernatant was again removed, and cells were resuspended, pelleted, and washed two additional times. Stock solutions of the Ru complexes were prepared in DMSO and diluted in PBS to a final DMSO concentration of <1% prior to use. Each compound was then added to aliquots of the 10-fold suspension of diluted blood. PBS was used as a negative control and a zero-hemolysis marker. A 1% sample of Triton X served as the positive control and the 100% lysis marker. All samples were placed in a shaking incubator (37°C, 200 rpm) for 1 hour. After mixing, the samples were centrifuged for 10 minutes at 10,000 rpm and the resulting supernatant was diluted by a factor of 4 using distilled water. The absorbance of the supernatant was then measured at 540 nm where the relative percent lysis of the complexes was determined using the equation below.

$$\%\ Lysis = \frac{Abs_{compound}}{Abs_{Triton\ X}} \times 100$$

Results and discussion

Synthesis and Characterization

Since their first description in 1864 by Hugo Schiff,[46] numerous compounds have been prepared that contain the azomethine/imine functional group that bears his name, often becoming a staple of biologically-active molecules.[47] Given the biological activity of the free complexes, Schiff bases have also been explored as ligands for metal-based drugs or models for enzyme active sites.[48, 49] Since the functional group of a Schiff base contains an imine, this is ideally suited to coordinate to several metal centers, particularly ruthenium, given that imine-based ligands form stable coordination complexes.[50] To improve the antibacterial activity of the prepared compounds, we included a ferrocene moiety, given the success of previous antibacterial agents which contain ferrocene.[51] For the target compounds, the Schiff base ligands **L1**, **L2**, and **L3** were chosen as they will provide preliminary structure-activity relationships (SAR) for the absence or presence of an appended ferrocene, along with the impact of a phenyl bridge between the imine and the ferrocene.

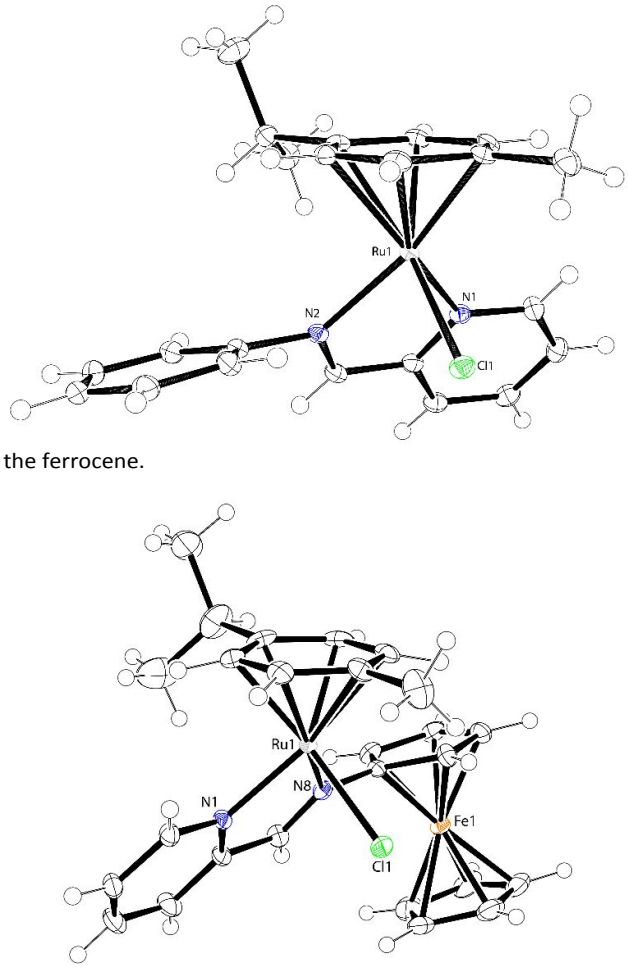

Figure 3. X-ray crystal structures of complexes **C1** (top) and **C3** (bottom), where the PF_6 anions and lattice solvent molecules are omitted for clarity. The ellipsoids of all non-hydrogen atoms are shown at the 50% probability level.

The complexes were prepared using a common scaffold of 2-pyridinecarboxaldehyde which underwent a condensation reaction with aniline, 4-ferrocenylaniline, and aminoferrocene to give the three Schiff base ligands. These ligands were then mixed with the Ru(II) dimer ([(*p*-cymene)$RuCl_2]_2$), followed by the addition of ammonium hexafluorophosphate to give our desired product as powders (**Figure 2**). To confirm the successful preparation of the target complexes, they were

characterized by ^{1}H and ^{13}C NMR (**Figures S1-S6**) where the diagnostic imine signals were observed. Additional validation was provided by elemental analysis and X-ray crystal structures which were determined for **C1** and **C3** (**Figure 3**). The crystals of **C1** contained a co-crystalizing acetone solvent molecule ($[(RuL_1)](PF_6)\bullet(CH_3)_2CO$), while for **C3** no solvent molecules were observed ($[RuL_3](PF_6)$).

For both **C1** and **C3** a similar half-sandwich coordination to the Ru metal center was observed, with the arene ring occupying one face of the molecule. The Schiff base ligand coordinates in a bidentate fashion through the pyridine and imine nitrogen atoms, while a single chloride completes the coordination sphere. Charge compensation is provided by a single hexafluorophosphate anion. Upon analysis, the Ru–N pyridine and Ru–N imine bond lengths were 2.085 Å and 2.100 Å respectively for **C1**. For **C3**, bond lengths of 2.080 Å and 2.066 Å were observed. Similar structures and bond lengths have been observed for previous Ru-arene complexes with bidentate chelating N,N donor ligands.[52, 53] Additionally, the crystal structure of **C1** is in good agreement with a structure from a similar Ru complex, having toluidine in the Schiff base ligand, that was prepared using a slightly different synthetic route.[54]

The pharmaceutical potential of ferrocene-based compounds has been well-established for a variety of applications.[55] The observed biological activity is frequently related to the oxidation of ferrocene to generate ferrocenium species that can promote the formation of reactive oxygen species (ROS).[56, 57] Therefore, to determine the redox potential of bound ferrocene in the studied systems, cyclic voltammetry (CV) experiments were performed (Table 1). For all three complexes, an irreversible peak was observed in the range of −0.61 to −0.80 V (Figures S7-S9). This behaviour is characteristic of a one-electron metal based oxidation of Ru(II) to Ru(III).[58] Another irreversible peak is observed at more negative potentials for all compounds. As shown in Table 1, this peak shifts positively (~400 mV) on addition of the ferrocene moiety in **C2** and **C3**. Furthermore, the absence of a reverse peak indicates an EC mechanism of electron transfer that corresponds to the Schiff base ligands. The positive shift in the reduction potential can be attributed to the electron donating character of the ferrocene ligands, which makes it easier to reduce the complex. In the case of complexes **C2** and **C3**, an additional reversible $Fe^{III/II}$ redox couple was observed (Figures S8 and S9). This difference of 0.20 V in the ferrocene couples of **C2** and **C3** indicates that the benzyl spacer makes it easier to oxidize the Fc group due to extended π-conjugation.

Aqueous Stability and Log D

Ruthenium-based therapeutics are often referred to as prodrugs, where the complexes are activated via ligand exchange, typically a labile chloride for a water molecule, which then facilitates coordination to their ultimate biological target.[59] For example, RAPTA-C undergoes rapid hydrolysis of a Ru–Cl bond at low chloride concentrations of 4–5 mM, forming the mono-aquated complex, $[Ru(p\text{-cymene})Cl(H_2O)(PTA)]^+$. However, at a 100 mM chloride ion concentration similar to that of blood, hydrolysis of the Ru–Cl bond is not observed.[60] RAPTA-C is therefore considered a pro-drug that is activated from its di-chlorido form just like cisplatin,[61] where exchange of one or two Cl^- ligands with water and the subsequent loss of the aqua ligand(s) allows the molecule to bind to its target. Similar to RAPTA-C, RM175 is also activated by ligand exchange of a chloride ligand with water at the monodentate site, thereby facilitating covalent binding to the N7 of guanine in the DNA double helix.[62]

To determine their aqueous stability, each complex was dissolved in PBS and incubated at 37 °C while UV-Vis spectra were measured over 6 hours. For all 3 complexes, no visible changes were observed, indicating that they have appreciable stability under physiological conditions (**Figures S10-S12**). A similar phenomenon was observed for previous Ru-arene Schiff base complexes, where negligible changes in the UV-Vis spectra occurred with prolonged incubation.[63]

Given the aforementioned impact of chloride ion concentration on hydrolysis, complementary analysis of the aqueous stability of the complexes was performed using ^{1}H NMR spectroscopy. For these measurements, the complexes were first mixed with deuterated DMSO, then subsequently diluted using D_2O. No buffering agents or salts were added to either deuterated solvent, thereby offering unimpeded ligand exchange opportunities. The samples were then incubated for 0, 1, 6, and 24 hours at 37 °C, after which ^{1}H NMR spectra were collected. Unsurprisingly, for all three compounds evidence of ligand exchange was observed. For **C1**, a clear yellow solution persisted, while new signals began to emerge in the ^{1}H NMR spectrum after 1 hour of incubation (**Figure S13**). A subtle

Complex	Ligand[a] *E* (V)	Ru[b] *E* (V)	Fc^+/Fc $E_{1/2}$ (V)	log $D_{7.4}$	K_{sv} (x 10^4 M^{-1})	log K
C1	−1.23	−0.80		0.062	2.1	4.32
C2	−0.85	−0.61	+0.12	0.89	4.1	4.61
C3	−0.87	−0.63	+0.32	0.16	3.2	4.51

Table 1. Results from the Stern-Volmer analysis, HSA titration, partitioning and cyclic voltammetry. Stern-Volmer quenching constant, K_{sv}, Binding Constants, K_b the partitioning of the complexes, and redox potentials (V vs Fc+/Fc).
[a]The reported potentials denote irreversible reduction of the Schiff base ligand.
[b]The potentials denote a one-electron irreversible oxidation of Ru(II) to Ru(III). No reverse wave is observed for the $Ru^{ii/iii}$ species.

increase in the signals was observed with continued incubation, however, these remained a minor species overall. Comparatively, for **C2** solubility of the parent compound was a significant problem, while substantial precipitation was observed for **C3** after only 1 hour of incubation resulting in minimal signals in the ^{1}H spectra (**Figure S15**). Therefore, the DMSO concentration was increased to 50%, which resulted in soluble species for the duration of the experiment. For both complexes, new signals emerged (**Figures S14 and S16**), however, similar to **C1**, these remained minor species overall. Taken together, these results confirm the impact of the chloride ions in the PBS suppressing exchange.

The ability of a therapeutic candidate to partition between aqueous and organic media is critical in determining their potential to diffuse across cell membranes.[64] To evaluate such distribution, the log $D_{7.4}$ for each complex was determined using the shake-flask method.[65] For these experiments, the complexes were combined with equal volumes of 1-octanol and PBS (pH 7.4), where the amount of the compounds within the aqueous layer were monitored before and after mixing by measuring its UV-Vis spectrum. Although the Ru compounds are complex ions, they all displayed a preference for the hydrophobic medium. Overall, the measured log $D_{7.4}$ values correlate well with decreasing polarity where the inclusion of the ferrocene increased the lipophilicity, as **C1** had the smallest lipophilicity with 0.062, **C3** was slightly higher with 0.16, while **C2** had the largest at 0.89. Previous RAPTA complexes observed that a more positive log P_{OW} (similar to Log D) correlated with a more cytotoxic Ru complex, likely due to the ability to passively diffuse across cell membrances.[66]

Binding to Human Serum Albumin

Human serum albumin (HSA) is the most abundant protein in blood and a known transporter for a variety of small molecules and therapeutics.[67] Previously successful Ru anticancer complexes have been observed to readily form non-coordinate interactions with the protein under physiological conditions (pH 7.4, 37 °C).[68, 69] Such interactions have been suggested to increase the bioavailability of the complexes, improving the aqueous solubility of hydrophobic therapeutics while also offering delivery to their site of action.[70, 71] For RM175, improved anticancer activity towards several cell lines when administered in the presence of albumin,[72] highlighting the importance of such interactions for Ru-arene complexes. Indeed, previous Ru-arene antibacterial complexes with thiosemicarbazone ligands were observed to bind to HSA with strong affinity,[73] which was proportional to the observed antibacterial activity.[74]

HSA contains a single tryptophan residue (Trp-214) which is responsible for the intrinsic fluorescence of the protein. This fluorescence can be attenuated due to changes in the local environment caused by small molecules entering the hydrophobic pocket where the tryptophan is located.[75] Measuring the relative extent of this quenching has provided significant insight into the affinity of HSA for various small molecules, including Ru(II)-arene complexes.[76] To determine the binding affinity of each complex for HSA, increasing amounts of each complex were mixed with a standard solution of HSA followed by incubation for 1 hour at 37 °C, after which fluorescence measurements were taken.

For all three complexes, a decrease in the fluorescence was observed (**Figures S17-S19**). This fluorescence quenching was quantified using the Stern-Volmer equation,

$$\frac{F_o}{F} = K_{SV}[Q] + 1$$

where F_o and F are the fluorescence intensities in the absence and presence of the quencher (Ru complex) respectively, K_{SV} is the Stern-Volmer quenching constant, and [Q] is the concentration of the quenching complex. From the above equation, a plot of F_o/F against the concentration of each complex yielded a linear relationship (**Figure 4**), where the slope was equal to the value of K_{sv}. The observed binding constants of the 3 complexes to HSA are summarized in **Table 1**, where **C2** > **C3** > **C1**. This result correlates with their partition coefficients (log $D_{7.4}$), indicating that **C2** had the greatest affinity for the hydrophobic binding pockets of the serum protein.

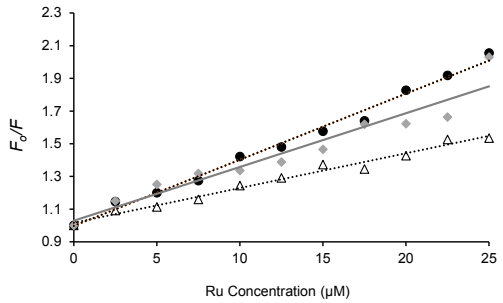

Figure 4. Stern–Volmer plot of fluorescence competition experiments for **C1** (△), **C2** (●), and **C3** (◆). Experimental conditions: [HSA] = 10 μM, [**C1**-**C3**] = 0–25 μM; excitation wavelength = 280 nm; emission wavelength maxima = 306 nm; ambient temperature; pH 7.4.

The ability of all three complexes to substantially quench the fluorescence of Trp-214 indicates that all the complexes associate with HSA in proximity to the residue, within the Sudlow binding site I,[77, 78] which could improve the bioavailability of the complexes. Furthermore, the observed binding affinities are similar to other Ru(II)-arene complexes.[79, 80] To determine the mechanism of quenching involved, the UV-Vis spectra of HSA in the absence and presence of each complex were measured. Overall, the absorption intensity of HSA decreased with no shift observed in the position of the absorption bands (**Figures S20-S22**), indicating that the fluorescence quenching was via a dynamic mechanism.[81]

Binding to DNA

DNA is often the primary pharmacological target for metal-based drugs, in particular the platinum-based anticancer compounds cisplatin, carboplatin, and oxaliplatin.[82] The predominant modes of interaction for metal-based complexes

with DNA are direct coordinate bonds, commonly via guanine residues, or through intermolecular interactions resulting in intercalation.[83-85] For RM175, the arene moiety has been observed to enhance hydrophobic interactions with DNA via arene-intercalation between DNA base pairs.[86] Previous Ru-arene antibacterial complexes with Schiff base ligands have observed DNA binding to readily occur in solution via intercalation.[87, 88] For such compounds, inducing DNA damage has been suggested to be an important part aspect of the mechanism of action, [89, 90] therefore the interactions between our complexes and DNA was investigated.

To determine the potential association between the prepared Ru complexes and DNA, each complex was first mixed with an equimolar amount of CT-DNA and the UV-Vis spectra were collected over 6 hours. For both **C1** and **C2** minimal changes were observed, suggesting that there were no coordinate interactions (**Figures S23 and S24**). By contrast, **C3** saw a hypochromic effect for the peak at 260 nm, along with a bathochromic shift in the peak at 350 nm (**Figure S25**). These changes signify substantial interactions occurred with the CT-DNA.

To further evaluate the association of the complexes with DNA titration experiments were conducted. In each case, the concentration of the Ru complex remained constant, while the CT-DNA concentration was gradually increased. The samples were incubated at 37 °C for 1 hour, then their UV-Vis spectra were collected. As observed above, the spectra for **C1** and **C2** were virtually unchanged with only a minor hypochromic effect observed (**Figure S26** and **Figure 5**), even with 3 equivalents of excess DNA. Comparatively, the spectra for **C3** saw a hyperchromic effect following the addition of variable equivalents of DNA (**Figure S28**). Comparing the λ_{max} following the addition of CT-DNA a bathochromic shift was observed for all 3 complexes; however, for **C1** and **C2** this was a minor change relative to **C3**. This is an interesting contrast, and likely the result of the absence of an additional phenyl spacer between the ferrocene and pyridine within the Schiff base ligand impacting the association of the complexes with the DNA. This was pronounced for **C3**, which also had the unique hyperchromic effect within the spectra.

The resulting binding constants for each complex with the CT-DNA were determined to quantitatively compare the binding strengths of the complexes using equation 2. The K_b values for the complexes are summarized in **Table 2** and reveal that **C2** > **C3** > **C1** in binding to CT-DNA. This is an identical pattern to the binding to HSA, with more hydrophobic complexes having a greater affinity. The binding constants for all three complexes are within the range of similar complexes for DNA intercalation, while being similar to those observed for previous Ru(II) complexes[81, 91, 92] and Ru(III) Schiff base complexes as well.[87] The observed hyperchromism of **C3** has also been observed for previous Ru(II)-arene complexes which also displayed a blue shift in the UV-Vis spectra, an observation that was attributed to electrostatic interactions with the CT-DNA.[93]

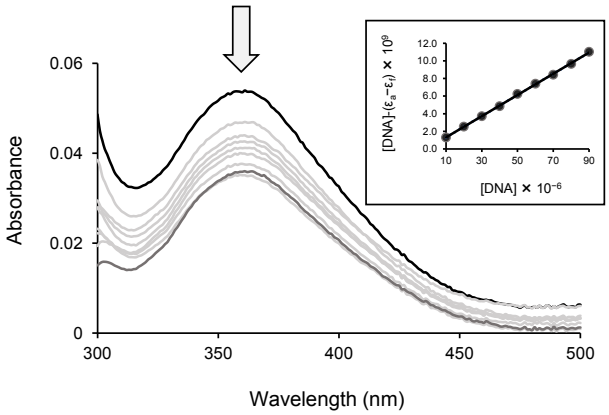

Figure 5. UV-Vis spectra of complex **C2** (30 μM) with CT-DNA (0–90 μM) in Tris-HCl buffer (pH 7.0) after 1 hour of incubation at 37 °C. Inset: Plot of [DNA] / (ε_A – ε_F) versus [DNA] for the titration of **C2** with CT-DNA.

Complex	λ_{max} (free)	λ_{max} (bound)	Δλ/nm	K_b / 10^5 M^{-1}
C1	313	314	2	2.9
C2	360	361	1	11
C3	334	342	8	8.2

Table 2. DNA-binding data for the Ru complexes following the CT-DNA titration.

Antibacterial Activity

The antibacterial activity of the Ru complexes was determined using a standard MIC assay. Overall 7 different Gram-positive bacterial strains were chosen based upon their prevalence in clinical bacterial infections.[94] The results of the MIC assay are summarized in **Table 3**. Surprisingly, **C1** and **C3** displayed no activity towards any of the strains, with bacterial growth observed even at the highest concentration evaluated (128 μg/mL). By contrast, **C2** displayed significant activity towards *S. aureus* (ATCC 25923), *S. epidermidis* (ATCC 51625), and *E. faecalis* (ATCC 51299) with an MIC of 8 μg/mL against each bacterial cell line. Additionally, an MIC of 16 μg/mL was observed for **C2** against one strain of MRSA (ATCC 33591), while an MIC of 128 μg/mL was observed towards the multidrug resistant MRSA strain (ATCC BAA-44). Using these results, SAR can be determined where the importance of the phenyl group bridging the Schiff base imine to the appended ferrocene, was evidently critical in the activity of **C2**, as both the absence of ferrocene in **C1**, or this phenyl spacer for **C3**, negated antibacterial activity. With the FDA standard for activity being 1 μg/mL, as observed for our positive controls, **C2** emerged as a promising therapeutic candidate.

Previously reported bioactive Fc complexes have attributed their cytotoxicity to the formation of reactive oxygen species (ROS),[56, 57] where oxidation of the Fc to Fc^+ is responsible for the observed biological activity. Accordingly, cathodic shifts in the oxidation potential of Fc can be correlated to higher bactericidal activity, as a lower thermodynamic barrier for Fc oxidation

Strain	C1	C2	C3	linezolid	amikacin
S. aureus (ATCC 25923)	> 128	8	> 128	1	NT
MRSA (ATCC 33591)	> 128	16	> 128	1	NT
MRSA (ATCC BAA-44)	> 128	128	> 128	1	NT
S. epidermidis (ATCC 51625)	> 128	8	> 128	1	NT
E. faecalis (ATCC 51299)	> 128	8	> 128	1	NT
P. aeruginosa (ATCC 27853)	> 128	> 128	> 128	NT	4
A. baumannii (ATCC 19606)	> 128	> 128	> 128	NT	8

Table 3. MIC values against clinically relevant bacterial strains for each Ru complex.
nt = not tested. All MIC values in μg/mL.

translates to more rapid ROS formation. Based on the above CV studies, it is intuitive that **C2** should correspond to greater antibacterial activity because of the lower anodic potential required to oxidize ferrocene. Indeed, upon comparing the observed MIC to the $E_{1/2}$ (Fc^+/Fc), it was the complex with the Fc that was easier to oxidize that had greater bactericidal activity. A similar correlation was observed for previous Ru-arene-Fc compounds,[33] suggesting that the mechanism of action of **C2** involves ROS generation.

Comparing the antibacterial activity of our Ru complexes to similar other Ru(II) compounds provides some additional context for the observed efficacy. First, the Ru(II)-arene dimer starting material was shown to be inactive against a variety of bacterial strains, while RAPTA-C displayed moderate activity.[95] A photoactive Ru(II) complex with 4,4'-dimethoxy-2,2'-bipyridine ligands displayed an MIC of 12.5 ug/mL towards *S. aureus*,[96] while a similar Ru(II) complex containing N-phenyl-substituted diazafluorenes had an MIC of 6.25 μg/mL against MRSA.[90] Recently, a Ru(II) complex with a Schiff-base benzimidazole ligand demonstrated significant activity towards two resistant microbial strains, further supporting the use of ruthenium complexes as effective antimicrobial agents.[97] Taken together, the diverse activity of **C2** is encouraging where the observed MIC values are approaching therapeutic utility.

Red Blood Cell Homolysis

To determine the compatibility of the compounds in biological media, a red blood cell (RBC) hemolysis assay was performed using mechanically defibrinated sheep blood.[98] For the analysis, PBS buffer was used as a negative control while Triton X (1%) was used as the positive control. The relative impact of each complex on the lysis of RBCs was compared as the absorbance at 540 nm relative to that of the Triton X sample. At a 50 μM concentration, **C1** had a relative lysis of 13.6 %, **C2** was the lowest with 9.4 %, while **C3** had highest with 14.4 %. Since the MIC of **C2** which was 8 μg/mL or 10 μM, the observed lysis is minimal even at a concentration that was well beyond the therapeutic dose. With an admissible level of hemolysis of biological materials being 5%,[99] **C2** was evidently well tolerated by the RBCs exhibiting minimal hemoglobin release.

Conclusions

With the continued advancement of antibacterial resistance there is a great need for alternative approaches to combat this adaptable opponent. Ruthenium complexes are promising candidates, given their established anticancer activity, where minimal side effects are commonly observed. To advance the field of ruthenium antibacterial agents, three Ru(II)-arene complexes with Schiff base ligands were prepared and evaluated to determine SAR.

Under physiological conditions in aqueous solution (pH 7.4, 37 °C), the complexes displayed pronounced stability, while also having a preference to partition into non-polar media. Modest binding to HSA and CT-DNA was also observed for all three compounds, where a consistent trend of coordination was observed where **C2** > **C3** > **C1**. Surprisingly, **C1** and **C3** were ineffective at preventing bacterial growth, while **C2** displayed a broad spectrum of activity, inhibiting growth of several medicinally relevant bacterial strains. In particular, a MIC of 8 μg/mL against *S. aureus*, and an MIC of 16 μg/mL towards MRSA. Furthermore, **C2** displayed low hemolytic release of RBC, suggesting it has good biological tolerance. Taken together, the SAR identified the importance of incorporating the ferrocene into the Schiff base ligand, while a phenyl linker was also required to bridge the imine to the ferrocene to ensure activity. The results of this study have identified **C2** as a promising candidate for further advancement.

Author Contributions

MIW designed the study and wrote the initial draft of the manuscript, while all authors were involved in reviewing and editing the manuscript. SM synthesized the Ru compounds and collected the UV-Vis and fluorescence data. MD measured the CV of the complexes. TB assisted with the Log $D_{7.4}$ measurements. CGH solved

the crystal structure for **C1** and GMF solved the crystal structure for **C3**. JDR and JJM performed the MIC and RBC hemolysis assay.

Conflicts of interest

There are no conflicts to declare.

Acknowledgements

The authors would like to thank the NSF (Grant numbers CHE-0722385 and CHE-1337497) for funding the 400 and 500 MHz NMR spectrometers at Illinois State University. The authors are also grateful to Dr Ellen Matson for her assistance with the cyclic voltammetry measurements. JJM and MIW thank the Illinois State University Chemistry Department for funding.

References

1. H. C. Neu, *Science*, 1992, **257**, 1064-1073.
2. G. M. Rossolini, F. Arena, P. Pecile and S. Pollini, *Curr. Opin. Pharmacol.*, 2014, **18**, 56-60.
3. CDC, Antibiotic Resistance Threats in the United States 2019, https://www.cdc.gov/drugresistance/pdf/threats-report/2019-ar-threats-report-508.pdf).
4. N. V. Loginova, H. I. Harbatsevich, N. P. Osipovich, G. A. Ksendzova, T. V. Koval'chuk and G. I. Polozov, *Current Medicinal Chemistry*, 2020, **27**, 5213-5249.
5. S. Waxman and K. C. Anderson, *Oncologist*, 2001, **6**, 3-10.
6. M. F. Hughes, B. D. Beck, Y. Chen, A. S. Lewis and D. J. Thomas, *Toxicol. Sci.*, 2011, **123**, 305-332.
7. B. Rosenberg, L. Vancamp and T. Krigas, *Nature*, 1965, **205**, 698-699.
8. S. Ghosh, *Bioorg. Chem.*, 2019, **88**.
9. S. P. Fricker, *Dalton Trans*, 2007, 43, 4903-4917.
10. A. Frei, J. Zuegg, A. G. Elliott, M. Baker, S. Braese, C. Brown, F. Chen, C. G. Dowson, G. Dujardin, N. Jung, A. P. King, A. M. Mansour, M. Massi, J. Moat, H. A. Mohamed, A. K. Renfrew, P. J. Rutledge, P. J. Sadler, M. H. Todd, C. E. Willans, J. J. Wilson, M. A. Cooper and M. A. T. Blaskovich, *Chem. Sci.*, 2020, **11**, 2627-2639.
11. J. Reedijk, *Platinum Metals Review*, 2008, **52**, 2-11.
12. S. Thota, D. A. Rodrigues, D. C. Crans and E. J. Barreiro, *J. Med. Chem.*, 2018, **61**, 5805-5821.
13. A. R. Simovic, R. Masnikosa, I. Bratsos and E. Alessio, *Coord. Chem. Rev.*, 2019, **398**, 113011.
14. A. F. A. Peacock and P. J. Sadler, *Chem.-Asian J.*, 2008, **3**, 1890-1899.
15. S. J. Dougan and P. J. Sadler, *Chimia*, 2007, **61**, 704-715.
16. R. E. Morris, R. E. Aird, P. D. Murdoch, H. M. Chen, J. Cummings, N. D. Hughes, S. Parsons, A. Parkin, G. Boyd, D. I. Jodrell and P. J. Sadler, *J. Med. Chem.*, 2001, **44**, 3616-3621.
17. Z. Adhireksan, G. E. Davey, P. Campomanes, M. Groessl, C. M. Clavel, H. J. Yu, A. A. Nazarov, C. H. F. Yeo, W. H. Ang, P. Droge, U. Rothlisberger, P. J. Dyson and C. A. Davey, *Nat. Commun.*, 2014, **5**.
18. Y. K. Yan, M. Melchart, A. Habtemariam and P. J. Sadler, *Chem. Comm.*, 2005, 4764-4776.
19. C. S. Allardyce, P. J. Dyson, D. J. Ellis and S. L. Heath, *Chem. Comm.*, 2001, 1396-1397.
20. P. J. Dyson, *Chimia*, 2007, **61**, 698-703.
21. S. Swaminathan, J. Haribabu, N. Balakrishnan, P. Vasanthakumar and R. Karvembu, *Coord. Chem. Rev.*, 2022, **459**, 214403.
22. B. S. Murray, M. V. Babak, C. G. Hartinger and P. J. Dyson, *Coord. Chem. Rev.*, 2016, **306**, 86-114.
23. C. Scolaro, A. Bergamo, L. Brescacin, R. Delfino, M. Cocchietto, G. Laurenczy, T. J. Geldbach, G. Sava and P. J. Dyson, *J. Med. Chem.*, 2005, **48**, 4161-4171.
24. A. Weiss, R. H. Berndsen, M. Dubois, C. Muller, R. Schibli, A. W. Griffioen, P. J. Dyson and P. Nowak-Sliwinska, *Chem. Sci.*, 2014, **5**, 4742-4748.
25. F. F. Li, J. G. Collins and F. R. Keene, *Chem. Soc. Rev.*, 2015, **44**, 2529-2542.
26. M. R. Gill and J. A. Thomas, *Chem. Soc. Rev.*, 2012, **41**, 3179-3192.
27. A. Singh and P. Barman, *Top. Curr. Chem.*, 2021, **379**.
28. C. Biot, G. Glorian, L. A. Maciejewski, J. S. Brocard, O. Domarle, G. Blampain, P. Millet, A. J. Georges, H. Abessolo, D. Dive and J. Lebibi, *J. Med. Chem.*, 1997, **40**, 3715-3718.
29. A. Nguyen, A. Vessieres, E. A. Hillard, S. Top, P. Pigeon and G. Jaouen, *Chimia*, 2007, **61**, 716-724.
30. G. Jaouen, A. Vessieres and S. Top, *Chem. Soc. Rev.*, 2015, **44**, 8802-8817.
31. M. Patra and G. Gasser, *Nature Reviews Chemistry*, 2017, **1**.
32. A. Kondratskyi, K. Kondratska, F. V. Abeele, D. Gordienko, C. Dubois, R.-A. Toillon, C. Slomianny, S. Lemiere, P. Delcourt, E. Dewailly, R. Skryma, C. Biot and N. Prevarskaya, *Scientific Reports*, 2017, **7**.
33. C. H. Mu, K. E. Prosser, S. Harrypersad, G. A. MacNeil, R. Panchmatia, J. R. Thompson, S. Sinha, J. J. Warren and C. J. Walsby, *Inorg. Chem.*, 2018, **57**, 15247-15261.
34. S. Goggins, E. A. Apsey, M. F. Mahon and C. G. Frost, *Organic & Biomolecular Chemistry*, 2017, **15**, 2459-2466.
35. P. Hu, K.-Q. Zhao and H.-B. Xu, *Molecules*, 2001, **6**, M249.
36. H. Ping, K.-Q. Zhao and H.-B. Xu, *Molecules*, 2001, **6**, M250.
37. Y. W. Dong, R. Q. Fan, X. M. Wang, P. Wang, H. J. Zhang, L. G. Wei, Y. Song, X. Du, W. Chen and Y. L. Yang, *Eur. J. Inorg. Chem.*, 2016, 3598-3610.
38. E. M. Njogu, B. Omondi and V. O. Nyamori, *S. Afr. J. Chem.*, 2016, **69**, 51-66.
39. V. C. Gibson, C. M. Halliwell, N. J. Long, P. J. Oxford, A. M. Smith, A. J. P. White and D. J. Williams, *Dalton Trans*, 2003, 918-926.
40. N. Chadwick, D. K. Kumar, A. Ivaturi, B. A. Grew, H. M. Upadhyaya, L. J. Yellowlees and N. Robertson, *Eur. J. Inorg. Chem.*, 2015, 4878-4884.
41. M. E. Reichmann, S. A. Rice, C. A. Thomas and P. Doty, *J. Am. Chem. Soc.*, 1954, **76**, 3047-3053.
42. J. Marmur, *Journal of Molecular Biology*, 1961, **3**, 208-218.
43. A. M. Pyle, J. P. Rehmann, R. Meshoyrer, C. V. Kumar, N. J. Turro and J. K. Barton, *J. Am. Chem. Soc.*, 1989, **111**, 3051-3058.
44. A. Wolfe, G. H. Shimer and T. Meehan, *Biochemistry*, 1987, **26**, 6392-6396.
45. CLSI, *Methods for Dilution Antimicrobial Susceptibility Tests for Bacteria That Grow Aerobically; Approved Standard - Eleventh Edition.*, Wayne, PA, USA.
46. H. Schiff, *Ann. Chem. Pharm.*, 1864, **131**, 118-119.

47. A. Kajal, S. Bala, S. Kamboj, N. Sharma and V. Saini, *J. Catal.*, 2013, 893512, 893515 pp.
48. A. Hameed, M. al-Rashida, M. Uroos, S. A. Ali and K. M. Khan, *Expert Opinion on Therapeutic Patents*, 2017, **27**, 63-79.
49. A. Erxleben, *Inorganica Chimica Acta*, 2018, **472**, 40-57.
50. E. A. Seddon and K. R. Seddon, *The Chemistry of Ruthenium*, Elsevier, Amsterdam; New York, 1984.
51. B. S. Ludwig, J. D. G. Correia and F. E. Kuhn, *Coord. Chem. Rev.*, 2019, **396**, 22-48.
52. S. K. Mandal and A. R. Chakravarty, *Polyhedron*, 1992, **11**, 823-827.
53. J. M. Gichumbi, H. B. Friedrich and B. Omondi, *Inorganica Chimica Acta*, 2017, **456**, 55-63.
54. T. S. Ramos, D. M. Luz, R. D. Nascimento, A. K. Silva, L. M. Liao, V. M. Miranda, V. M. Deflon, M. P. de Araujo, L. T. Ueno, F. B. C. Machado, L. R. Dinelli and A. L. Bogado, *Journal of Organometallic Chemistry*, 2019, **892**, 51-65.
55. S. Peter and B. A. Aderibigbe, *Molecules*, 2019, **24**.
56. D. Osella, M. Ferrali, P. Zanello, F. Laschi, M. Fontani, C. Nervi and G. Cavigiolio, *Inorganica Chimica Acta*, 2000, **306**, 42-48.
57. G. Tabbi, C. Cassino, G. Cavigiolio, D. Colangelo, A. Ghiglia, I. Viano and D. Osella, *J. Med. Chem.*, 2002, **45**, 5786-5796.
58. E. Reisner, V. B. Arion, M. F. C. Guedes Da Silva, R. Lichtenecker, A. Eichinger, B. K. Keppler, V. Y. Kukushkin and A. J. L. Pombeiro, *Inorg. Chem.*, 2004, **43**, 7083-7093.
59. S. Y. Lee, C. Y. Kim and T. G. Nam, *Drug Des. Dev. Ther.*, 2020, **14**, 5375-5392.
60. C. Scolaro, C. G. Hartinger, C. S. Allardyce, B. K. Keppler and P. J. Dyson, *J. Inorg. Biochem.*, 2008, **102**, 1743-1748.
61. C. Artner, H. U. Holtkamp, C. G. Hartinger and S. M. Meier-Menches, *J. Inorg. Biochem.*, 2017, **177**, 322-327.
62. F. Wang, H. M. Chen, S. Parsons, I. D. H. Oswald, J. E. Davidson and P. J. Sadler, *Chem. Eur. J.*, 2003, **9**, 5810-5820.
63. M. J. Chow, C. Licona, D. Y. Q. Wong, G. Pastorin, C. Gaiddon and W. H. Ang, *J. Med. Chem.*, 2014, **57**, 6043-6059.
64. L. Z. Benet, C. M. Hosey, O. Ursu and T. I. Oprea, *Advanced Drug Delivery Reviews*, 2016, **101**, 89-98.
65. OECD, *Test #107: Partition Coefficient (n-octanol/water): Shake Flask Method*, OECD Publishing, 1995.
66. A. K. Renfrew, L. Juillerat-Jeanneret and P. J. Dyson, *Journal of Organometallic Chemistry*, 2011, **696**, 772-779.
67. D. Sleep, *Expert Opinion on Drug Delivery*, 2015, **12**, 793-812.
68. N. Cetinbas, M. I. Webb, J. A. Dubland and C. J. Walsby, *J. Biol. Inorg. Chem.*, 2010, **15**, 131-145.
69. M. I. Webb and C. J. Walsby, *Dalton Trans*, 2011, **40**, 1322-1331.
70. M. I. Webb, R. A. Chard, Y. M. Al-Jobory, M. R. Jones, E. W. Y. Wong and C. J. Walsby, *Inorg. Chem.*, 2012, **51**, 954-966.
71. M. I. Webb, B. Wu, T. Jang, R. A. Chard, E. W. Y. Wong, M. Q. Wong, D. T. T. Yapp and C. J. Walsby, *Chem. Eur. J.*, 2013, **19**, 17031-17042.
72. A. Bergamo, A. Masi, A. F. A. Peacock, A. Habtemariam, P. J. Sadler and G. Sava, *J. Inorg. Biochem.*, 2010, **104**, 79-86.
73. F. A. Beckford, A. Stott, A. Gonzalez-Sarrias and N. P. Seeram, *Appl. Organomet. Chem.*, 2013, **27**, 425-434.
74. G. Devagi, F. Dallemer, P. Kalaivani and R. Prabhakaran, *Journal of Organometallic Chemistry*, 2018, **854**, 1-14.
75. F. Yang, Y. Zhang and H. Liang, *Int. J. Mol. Sci.*, 2014, **15**, 3580-3595.
76. S. Hairat and M. Zaki, *Journal of Organometallic Chemistry*, 2021, **937**.
77. G. Sudlow, D. J. Birkett and D. N. Wade, *Molecular Pharmacology*, 1975, **11**, 824-832.
78. S. Sugio, A. Kashima, S. Mochizuki, M. Noda and K. Kobayashi, *Protein Eng.*, 1999, **12**, 439-446.
79. O. A. Lenis-Rojas, M. P. Robalo, A. I. Tomaz, A. R. Fernandes, C. Roma-Rodrigues, R. G. Teixeira, F. Marques, M. Folgueira, J. Yanez, A. A. Gonzalez, M. Salamini-Montemurri, D. Pech-Puch, D. Vazquez-Garcia, M. L. Torres, A. Fernandez and J. J. Fernandez, *Inorg. Chem.*, 2021, **60**, 2914-2930.
80. L. Colina-Vegas, K. M. Oliveira, B. N. Cunha, M. R. Cominetti, M. Navarro and A. A. Batista, *Inorganics*, 2018, **6**.
81. D. Gopalakrishnan, M. Ganeshpandian, R. Loganathan, N. S. P. Bhuvanesh, X. J. Sabina and J. Karthikeyan, *Rsc Advances*, 2017, **7**, 37706-37719.
82. J. Zhou, Y. Kang, L. Chen, H. Wang, J. Liu, S. Zeng and L. Yu, *Frontiers in Pharmacology*, 2020, **11**.
83. A. M. Pizarro and P. J. Sadler, *Biochimie*, 2009, **91**, 1198-1211.
84. J. Carlos Garcia-Ramos, R. Galindo-Murillo, F. Cortes-Guzman and L. Ruiz-Azuara, *Journal of the Mexican Chemical Society*, 2013, **57**, 245-259.
85. H. K. Liu and P. J. Sadler, *Accounts of Chemical Research*, 2011, **44**, 349-359.
86. O. Novakova, H. M. Chen, O. Vrana, A. Rodger, P. J. Sadler and V. Brabec, *Biochemistry*, 2003, **42**, 11544-11554.
87. M. A. Malik, M. K. Raza, O. A. Dar, Amadudin, M. Abid, M. Y. Wani, A. S. Al-Bogami and A. A. Hashmi, *Bioorg. Chem.*, 2019, **87**, 773-782.
88. M. R. Kollipara, L. Shadap, V. Banothu, N. Agarwal, K. M. Poluri and W. Kaminsky, *Journal of Organometallic Chemistry*, 2020, **915**.
89. K. A. Kumar, K. L. Reddy, S. Vidhisha and S. Satyanarayana, *Appl. Organomet. Chem.*, 2009, **23**, 409-420.
90. P. L. Lam, G. L. Lu, K. M. Hon, K. W. Lee, C. L. Ho, X. Wang, J. C. O. Tang, K. H. Lam, R. S. M. Wong, S. H. L. Kok, Z. X. Bian, H. Li, K. K. H. Lee, R. Gambari, C. H. Chui and W. Y. Wong, *Dalton Trans*, 2014, **43**, 3949-3957.
91. L. L. Li, W. Q. Cao, W. J. Zheng, C. D. Fan and T. F. Chen, *Dalton Trans*, 2012, **41**, 12766-12772.
92. M. Ganeshpandian, R. Loganathan, E. Suresh, A. Riyasdeen, M. A. Akbarsha and M. Palaniandavar, *Dalton Trans*, 2014, **43**, 1203-1219.
93. R. K. Gupta, R. Pandey, G. Sharma, R. Prasad, B. Koch, S. Srikrishna, P. Z. Li, Q. Xu and D. S. Pandey, *Inorg. Chem.*, 2013, **52**, 3687-3698.
94. A. S. Lee, H. de Lencastre, J. Garau, J. Kluytmans, S. Malhotra-Kumar, A. Peschel and S. Harbarth, *Nature Reviews Disease Primers*, 2018, **4**.
95. C. S. Allardyce, P. J. Dyson, D. J. Ellis, P. A. Salter and R. Scopelliti, *Journal of Organometallic Chemistry*, 2003, **668**, 35-42.
96. R. F. Donnelly, N. C. Fletcher, P. J. McCague, J. Donnelly, P. A. McCarron and M. M. Tunney, *Letters in Drug Design & Discovery*, 2007, **4**, 175-179.

97. V. P. Sur, A. Mazumdar, P. Kopel, S. Mukherjee, P. Vitek, H. Michalkova, M. Vaculovicova and A. Moulick, *Int. J. Mol. Sci.*, 2020, **21**.
98. Z. G. Liu, A. Brady, A. Young, B. Rasimick, K. Chen, C. H. Zhou and N. R. Kallenbach, *Antimicrob. Agents Chemother.*, 2007, **51**, 597-603.
99. M. K. M. Subarkhan and R. Ramesh, *Inorganic Chemistry Frontiers*, 2016, **3**, 1245-1255.